On the relationship between tight coevolution and superinfection

BU-1328-M

Carlos Castillo-Chavez

Biometrics Unit Cornell University Ithaca NY 14853-7801

and

Jorge X. Velasco-Hernández

Departamento de Matemáticas, UAM-Iztapalapa Apdo. Postal 55-534, Mexico D.F. 09340 MEXICO and Biometrics Unit, Cornell University

Abstract

The effects of density-dependence on the coevolution of virulence in superinfection models is the theme of this paper, The qualitative dynamics of three host-pathogen systems are studied numerically in a virulence-superinfection parameter landscape. It is shown numerically that pathogen's competitive exclusion, coexistence and host population extinction depend heavily on the population dynamics of the host population Reported patterns of diversity found using models without demography, are insufficient to account for the coevolutionary dynamics under defined selective pressures. Specifically, virulence and superinfection in the presence of a variable host population give rise to threshold values that divide (as switches) the regions of coexistence and competitive exclusion. Tight coevolution on a variable host population may occur within regions of parameter space that are not connected. We present our numerical results using a simple host-disease system where a homogeneous host population is invaded by two competing pathogen strains (partial analytical results will be published elsewhere).

Keywords: Superinfection, competitive exclusion, evolution of virulence, theoretical ecology, mathematical epidemiology.

1. Introduction

Virulence v and superinfection σ are two of several factors capable of explaining the observed coexistence of pathogenic parasitic strains in host populations. The population dynamics of host populations may dramatically affect the likelihood of coexistence or pathogen diversity—as measured by the shape, size, and properties of regions in parameter space. We argue in this article that reported patterns of diversity found using models without demography, are insufficient to account for the coevolutionary dynamics under defined selective pressures. Specifically, virulence and superinfection in the presence of a variable host population give rise to threshold values that divide (as switches) the regions of coexistence and competitive exclusion. Tight coevolution (Janzen, 1980; Levin and Castillo-Chavez, 1988)on a variable host population may occur within regions of parameter space that are not connected.

We present our results using a simple host-disease system where a homogeneous host population is invaded by two competing pathogen strains. In general, in the absence of superinfection (here a measure of the competitive ability of the most virulent strain) competitive exclusion of one strain is the generic outcome (Bremerman and Thieme, 1989; Castillo-Chavez et al. 1995). Levin and Pimentel (1981) were the first to show that the inclusion of superinfection makes coexistence possible.

The results of this article are supported by extensive numerical simulations. The partial analysis of Model (1) can be found in May and Nowak (1994) while the partical analysis of Models (2) and (3) can be found in Mena-Lorca *et al.* (1995). The characterization of the qualitative effects of frequency- and density-dependent population dynamics on disease dynamics as a function of superinfection (σ) and virulence (v) is a rather formidable challenge. However, the numerical simulations of this article give a qualitative picture that seriously questions the value of using frequency and density-independent models to study the evolution of virulence.

2. Competitive systems and superinfection

Superinfection (σ), virulence (v) and demography are mechanisms responsible for the competitive exclusion and/or coexistence of two related pathogen strains. Existence and stability of equilibria are viewed as functions of virulence and superinfection in a two-dimensional parameter landscape in various situations.

It is known (Nowak and May, 1994; May and Nowak, 1994) that populations that do not change under demographic preassures can be characterized

in σ-v landscapes by connected regions of coexistence. However, the dynamics of populations subject to variability in density may be characterized by qualitatively different $\sigma - v$-landscapes. In this article we assume, following Bremerman and Thieme (1989) and Nowak and May (1994) that the reproductive numbers of each competing strain are convex functions of the virulence, specifically we let the per-capita infection rate $\beta_i = c_i v_i/(m + v_i)$ (with c_i and m parameters that regulate the concavity of of β_i as v_i changes), that is, an optimal value of the reproductive number associated with the survival of each competing strain is achieved at the virulence $v_i = v_i^* > 0$ for each strain, respectively. This (convexity) assumption supports coexistence (for populations with reproductive numbers satisfying $R_1 > R_2 > 1$) of strains with superoptimal virulences, that is, with virulences satisfying $v^* < v_1 < v_2$ (Bremerman and Thieme, 1989).

In the following sections we look at the shape and stability properties of regions of the σ-v landscape for various models. The models may have equilibrium points with both pathogen strains present. We call these 'coexistence' equilibria. However, 'coexistence' equilibria may be unstable or locally asymptotically stable.

2.1 Superinfection with constant population size

We review first qualitative properties of the two-strain version of the model used by May and Nowak (1994) and Tilman (1994). Let S, I_1 and I_2 represent the densities of hosts, infected individuals with strain 1, and 2, respectively. The equations that govern the dynamics of these variables are:

$$\begin{aligned} S' &= k - uS - \beta_1 S I_1 - \beta_2 S I_2, \\ I_1' &= \beta_1 S I_1 - \sigma \beta_2 I_2 I_1 - (u + v_1) I_1, \\ I_2' &= \beta_2 S I_2 + \sigma \beta_2 I_2 I_1 - (u + v_2) I_2, \end{aligned} \tag{1}$$

where k denotes the recruitment rate explicitly defined in May and Nowak (1994) by $k = u(I_1 + I_2) + v_1 I_1 + v_2 I_2$; β_i is the per capita infection rate associated with strain i; u is the natural mortality rate; and v_i is the virulence or disease-induced mortality due to type i pathogen. It is assumed that $v_2 > v_1$. Studies of this two-strain superinfection model or its generalizations have been carried out recently (see Nowak and May, 1994; May and Nowak, 1994; Tilman, 1994). Figure 1 shows the region of coexistence predicted by the constant population size Model (1) of May, Nowak and Tilman. All parameters are fixed except σ and v_2.

The main features of the $\sigma - v$-landscape are:

1. An increase in superinfection (σ) widens the connected region of coexistence.
2. For large values of σ, the lower bound for the virulence v_2—below which coexistence is no longer possible— is practically constant.
3. For small values of σ a narrow band appears where coexistence is possible (only Figures 1 and 5).
4. The two regions of coexistence described in 2.) and 3.) can be clearly separated in the proximity of a value σ^* (in the case of the examples shown in Figures 1, 3 and 5 we have $\sigma^* \approx 0.5$).
5. In the region of coexistence R_0, the basic reproductive number of the disease (as a whole), is always greater than 1.

In this model, each pathogen's basic reproductive number is given by

$$R_i = \beta_i N/(u + v_i).$$

In the $\sigma - v$ landscape of Model (1), the region to the left of $\sigma^* = 0.5$ contains only unstable equilibria; the region to the right contains only asymptotically stable equilibrium points. In Figures 2.1 and 2.2 we show computer simulations of Model (1) for each of these cases. Figure 2.1 illustrates the case of a typical outcome in the region to the left of σ^*. Strain 2 eventually excludes strain 1 from the system regardless of the relatively high level of cross-immunity (measured by the small value of σ) that the latter induces in the host. To the right of σ^*, there is stable coexistence with strain 1 achieving higher prevalence than its competitor (as expected, the roles may shift as σ increases further).

In summary, the region of coexistence where the equilibria are asymptotically stable is connected and to the right of σ^*. To the left of σ^* competitive exclusion of the first strain takes place.

In the Appendix we write explicit formulae for the equilibria of (1).

2.2 Superinfection with constant recruitment

The inclusion of demographic dynamics in the host population produces regions of coexistence in parameter space that differ from those found in Nowak and May (1994; Figures 1 and 2). We introduce variability in the total population and hence, the contact rates that describe the infection process are now frequency dependent. The population dynamics are governed by the

following set of equations:

$$\begin{aligned} S' &= k - uS - \beta_1 SI_1/N - \beta_2 SI_2/N, \\ I_1' &= \beta_1 SI_1/N - \sigma\beta_2 I_2 I_1/N - (u+v_1)I_1, \\ I_2' &= \beta_2 SI_2/N + \sigma\beta_2 I_2 I_1/N - (u+v_2)I_2, \end{aligned} \tag{2}$$

where $N = S + I_1 + I_2$ and all other parameters are defined as before with k a fixed constant.

Model (2) with constant recruitment rate k (but variable population size) has the strain-specific basic reproductive rate given by (Bremermann and Thieme, 1989) as

$$R_i = k\beta_i/u(u+v_i).$$

In the absence of disease or when virulence is negligible ($v_i = 0$), the total population N tends asymptotically to the value k/u. In this case, Models (1) and (2) are equivalent. However, if virulence significantly affects the natural demographic processes in the host population the equivalence breaks down. Figure 3 shows the parameter landscape for this situation—N not constant. This landscape possesses the same features listed in the previous section except for item 3. To the right of σ^* ($\sigma^* \approx 0.5$), the upper bound of the coexistence region increases less steeply than in the previous case but it only contains asymptotically stable equilibrium points. However, for values of $\sigma < \sigma^*$, there is no coexistence region with asymptotic stability. In this region the total population becomes extinct. Thus, in the region where the constant population size model (1) predicts persistence of the disease (only a single strain present), the variable population model (2) predicts extinction of the host population. There is, therefore, a net reduction in the region where the disease may successfully (*e.g.* invade and remain in the host). In Figures 4.1 and 4.2 we present the asymptotic trends of the interaction. As expected for $\sigma < 1$ (induccion of cross-immunity) the first strain has higher prevalence. For $\sigma > 1$ (increased susceptibility to secondary infections), $I_2 > I_1$. In the Appendix we show explicitly the formulae for the equilibria in this case.

2.3 Superinfection with density-dependent mortality

A significative qualitative change in the region of coexistence is observed when density-dependent recruitment and mortality are assumed. Let X, Y_1 and Y_2 be the susceptible, infective hosts with strain 1 and infective hosts

with strain 2, respectively. The model that we use in this case is (see Mena-Lorca et al., 1995):

$$\begin{aligned} X' &= bN - \theta(N)X/N - \beta_1 XY_1/N - \beta_2 XY_2/N, \\ Y_1' &= \beta_1 XY_1/N - \sigma\beta_2 Y_2 Y_1/N - \theta(N)Y_1/N + v_1 Y_1, \\ Y_2' &= \beta_2 SY_2/N + \sigma\beta_2 Y_2 Y_1/N - \theta(N)Y_2/N + v_2 Y_2, \end{aligned} \tag{3}$$

where all parameters are defined as before except that $N = X + Y_1 + Y_2$, $\theta(N) \equiv (u + rN/K)N$ with $r = b - u$ the per-capita birth rate, and K the carrying capacity. Density-dependent mortality is proportional to the number of individuals in each compartment. Model (3) assumes logistic density-dependent mortality but our results are valid for more general functions (Mena-Lorca et al., 1995).

Using the rescaled variable variables

$$I_1 = \frac{Y_1}{N}, \quad I_2 = \frac{Y_2}{N}, \quad S = \frac{X}{N},$$

and

$$t = \tau/r, \quad \hat{\beta}_i = \beta_i/r, \quad \hat{v}_i = v_i/r, \quad \hat{u} = u/r, \quad \hat{N} = N/K,$$

we obtain the system:

$$\begin{aligned} I_1' &= \left(\hat{\beta}_1 S - \sigma\hat{\beta}_2 I_2 - \hat{u} - \hat{v}_1 - 1 + \hat{v}_1 I_1 + \hat{v}_2 I_2\right) I_1, \\ I_2' &= \left(\hat{\beta}_2 S + \sigma\hat{\beta}_2 I_1 - \hat{u} - \hat{v}_2 - 1 + \hat{v}_1 I_1 + \hat{v}_2 I_2\right) I_2, \\ \hat{N}' &= \left(1 - \hat{N} - \hat{v}_1 I_1 - \hat{v}_2 I_2\right)\hat{N}, \end{aligned} \tag{4}$$

where ($' = d/d\tau$). The basic reproductive numbers for each strain in Model (3) are

$$R_i = \beta_i/(r + u + v_i).$$

Both depend on the demographic parameter r. Figure 5 shows the parameter landscape for Equation (4). The area associated with coexistence is smaller relative to the range of values of σ and v_2 used in the two prior examples. Moreover, this region is qualitatively different. To the right of σ^* ($\sigma^* \approx 0.5$ in Figure 5), the upper bound of the region is roughly below the corresponding lower bound of the two previous cases; to the left of σ^*, the region of coexistence is wider than in Figure 1 but now it is a region of asymptotically stable equilibria. Competitive exclusion does not occur and the population does not become extinct. Figure 6.1 uses parameters in the region to the

left of σ^*. I_2 reaches higher prevalence than I_1 but cross-immunity support coexistence of both strains. To the right of σ^* the same trend observed in Model (2) occurs, namely density-dependence gives rise to a $\sigma - v$ parameter landscape with two disconnected regions where coexistence is stable.

3. Conclusions

Virulence and superinfection play an essential role on the tight coevolution of pathogens whose fate is intimately connected to that of the host (Levin and Pimentel, 1981; Mena-Lorca et al. 1995). Tight coevolution often has a dramatic effect on the long-term interaction of hosts and pathogens and, hence, it must be a key mechanism in the study of the evolution of virulence. Ignoring host demography reduces the effect of tight coevolution.

Mechanisms of patch generation and extinction (the selection factors) constitute the main difference among the models in Section 2. In Model(1) patch replacement is the only process capable of generating new patches. Extinction is crucially coupled with recruitment as there is no net increase or decrease in total number of patches. Model (2) assumes that external disturbances generate new patches (*cf.* Levin and Paine, 1974 and Paine and Levin, 1981). Disturbance (patch production represented by k) and patch extinction (represented by v_1 and v_2) are independent of each other. Model (3) assumes a feedback in patch production rate whereby new patches are produced as function of the total number of patches present. In Models (2) and (3) the total number of patches may increase or decrease depending upon the balance between patch generation and extinction (recruitment rate and virulence).

In the $v_2 - \sigma$ parameter landscape represented in Figures 1, 3 and 5, we can identify two main regions: one of low virulence-low superinfection (located in the lower left-hand side) and another of high virulence-high superinfection (upper right-hand side). In all cases the high virulence-high superinfection region contains asymptotically stable equilibria where both strains coexist. However, for patch production feedback and patch replacement models (Eq. (1) and (3) respectively) the corresponding low virulence-low superinfection regions have different properties. Model (1) supports the competitive exclusion of the inferior competitor occurs; Model(3) supports the coexistence of both strains. Apparently in this low virulence-low superinfection region, feedback production of patches increases diversity whereas replacement mechanisms produce monospecific epidemics. In Model (2)–external generation of patches–, this same parameter region cannot sustain a host population (the host is extinct).

Models designed to study the evolution of virulence of viruses such as HIV in terms of diversity indexes and superinfection (Nowak and May, 1994; May and Nowak, 1994) must evaluate their conclusions after the effects of tight coevolution have been incorporated through selective coefficients of recruitment, invasion and mortality.

In the ecological context Tilman (1994) developed a patch occupancy model to study coexistence patterns of species. His model shares the same mathematical structure of that of Nowak and May (1994) and assumes that the number of patches available for colonization is constant. If selection is going to play a role in this system, Tilman's assumption of a fixed number of patches demands (mathematically), instantaneous recruitment that compensate for the differences between colonization and extinction rates of each species.

The models described in this work are 'simple' in the sense that they have as few compartments as possible. They constitute the 'simplest' versions of the multicompartment models studied by Tilman (1994) and Nowak and May (1994). Their multicompartment models fall within the larger class of models often referred as metapopulation models. The analysis that supports the biological conclusions of Tilman and Nowak and May can be handled relatively straightforward because it assumes that each species or each host population is at equilibrium, that is, the total population size of host types (Nowak and May, 1994) or patches (Tilman, 1994) are unchanged throughout the process. The incorporation of selective effects makes the mathematical study of multispecies models for coevolution very difficult. However, simulations can be very useful in our qualitative study of multispecies models.

It is necessary to incorporate selective factorsto gain further understanding of the evolution of virulence. Spatial models are needed to better understand host-parasite coevolutionary interactions (Dwyer *et al.*, 1990). Models that take into account spatial heterogeneities may be fundamental for understanding plant-disease dynamics (Durret and Levin, 1994). However, while dealing with plant disease dynamics one must also consider the role of diffuse coevolution (Erlich and Raven, 1969) for which metapopulation models may be too simple of an approximation.

Acknowledgements This research has been funded by grant DEB-9253570 (Presidential Faculty Award) to Carlos Castillo-Chavez. This research was completed while JXVH was visiting fellow of the Royal Society of London/Academia de la Investigación Científica, at the Zoology Department of the University of Oxford. JXVH acknowledges the support of CONACYT grant 400200-5-3551E.

References

Hans J. Bremermann and Horst R. Thieme (1989) A competitive exclusion principle for pathogen virulence, *Journal of Mathematical Biology* 27:179–190.

Carlos Castillo-Chavez, Wenzhang Huang and Jia Li (1996) Dynamics of multiple pathogen strains in heterosexual epidemiological models, *Proceedings of the International Conference on Differential Equations Applied to Biology and Industry.* World Scientific, New Jersey.

Richard Durret and Simon A. Levin (1994) The importance of being discrete (and spatial). *Theoretical Population Biology* 46:363–394.

Greg Dwyer, Simon A. Levin and Linda Buttel (1990) A simulation model of the population dynamics and evolution of myxomatosis. *Ecological Monographs* 60:423–447.

P.R. Ehrlich and P.H. Raven (1969) Butterflies and plants: a study in coevolution. *Evolution* 18:596–608.

D.H. Janzen (1980) When is it coevolution? *Evolution* 34: 611–612.

Simon A. Levin and Carlos Castillo-Chavez (1988) Topics in evolutionary biology. In S. Lessard (editor): Mathematical and statistical developments in evolutionary theory, pp:327–358, NATO ASI series, Kluwer Academic, Boston.

Simon Levin and R. T. Paine (1974) Disturbance, patch formation and community structure, *Proceedings of the National Academy of Sciences USA* 71(7):2744–2747.

Simon Levin and David Pimentel (1981) Selection of intermediate rates of increase in parasite-host systems, *American Naturalist* 117(3):308–315.

Robert M. May and Martin N. Nowak (1994) Superinfection, metapopulation dynamics, and the evolution of virulence, *Journal of Theoretical Biology* 170:95–114.

Jaime Mena-Lorca, Jorge X. Velasco-Hernandez and Carlos Castillo-Chavez (1995) Superinfection, virulence and density-dependent mortality in an epidemic model. BU-1299 Biometrics Unit, Cornell University.

Martin N. Nowak and Robert M. May (1994) Superinfection and the evolution of parasite virulence, *Proceedings of the Royal Society of London* 255:81–89.

R.T. Paine and Simon A. Levin (1981) Intertidal landscape: disturbance and the dynamic of patterns, *Ecological Monographs* 51(2): 145–178.

.....10

David Tilman (1994) Competition and biodiversity in spatially structured habitats, *Ecology*: 75(1) 2–16.

Appendix

In this section we give the formulas that were used to compute the parameter landscapes of Figures 1, 3 and 5.

A.1 Equilibria of the constant size model (1)

For Model (1) the total population was rescaled to $N = 1$. Thus we have

$$I_1^* = \frac{-\left(\beta_2{}^2\, s\right) + \beta_1\, u - \beta_2\, u + \beta_2\, s\, u - \beta_2\, v_1 + \beta_1\, v_2 + \beta_2\, s\, v_2}{\beta_2\, s\, \left(\beta_1 - \beta_2 + \beta_2\, s\right)},$$

$$I_2^* = \frac{\beta_1\, \beta_2\, s - \beta_1\, u + \beta_2\, u - \beta_2\, s\, u + \beta_2\, v_1 - \beta_2\, s\, v_1 - \beta_1\, v_2}{\beta_2\, s\, \left(\beta_1 - \beta_2 + \beta_2\, s\right)}.$$

The stability analysis of these equilibria in a neighborhood of $\sigma = 1$ is given in May and Nowak (1994).

A.2 Equilibria of the constant recruitment model (2)

For Model (2) we use the equivalent system that inculdes the equation for the total population size N:

$$N'(t) = k - uN - v_1 I_1 - v_2 I_2,$$

and the equations for I_1 and I_2 given in (2). Of course we have $S = N - I_1 - I_2$. The formulae for the equilibrium densities are

$$N^* = \frac{\beta_2\, k\, \sigma\, \left(\beta_1 - \beta_2 + \beta_2\, \sigma\right)}{\left(\beta_2\, \sigma + v_1 - v_2\right)\, \left(\beta_1\, u - \beta_2\, u + \beta_2\, \sigma\, u - \beta_2\, v_1 + \beta_1\, v_2\right)},$$

$$I_1^* = \frac{k\, \left(\beta_2{}^2\, \sigma - \beta_1\, u + \beta_2\, u - \beta_2\, \sigma\, u + \beta_2\, v_1 - \beta_1\, v_2 - \beta_2\, \sigma\, v_2\right)}{\left(-\left(\beta_2\, \sigma\right) - v_1 + v_2\right)\, \left(\beta_1\, u - \beta_2\, u + \beta_2\, \sigma\, u - \beta_2\, v_1 + \beta_1\, v_2\right)},$$

$$I_2^* = -\frac{k\, \left(-\left(\beta_1\, \beta_2\, \sigma\right) + \beta_1\, u - \beta_2\, u + \beta_2\, \sigma\, u - \beta_2\, v_1 + \beta_2\, \sigma\, v_1 + \beta_1\, v_2\right)}{\left(\beta_2\, \sigma + v_1 - v_2\right)\, \left(\beta_1\, u - \beta_2\, u + \beta_2\, \sigma\, u - \beta_2\, v_1 + \beta_1\, v_2\right)}.$$

The local stability analysis of this model is not presented here since our objective is to compare different parameter landscapes and associated asymptotic dynamics. Extensive numerical explorations of the model were, however, performed to support our claims.

A.3 Equilibria of the density-dependent model (4)

Using the change of variables of section 2.3, the basic reproductive numbers of each strain are given by

$$R_i = \frac{\hat{\beta}_i}{1+\hat{u}+\hat{v}_i}.$$

Let

$$\Psi_1 = -\hat{\beta}_1 + \hat{\beta}_2(1-\sigma),\ \Psi_2 = \hat{v}_2 - \hat{v}_1 - \sigma\hat{\beta}_2.$$

Then the coexistence equilibrium points are given by

$$\Big(\frac{-(1+\hat{u})}{\Psi_2} + \frac{\hat{\beta}_2 - \hat{v}_2}{\Psi_1}, \frac{1+\hat{u}}{\Psi_2} + \frac{-\hat{\beta}_1 + \hat{v}_1}{\Psi_1}, \hat{N}^*\Big),$$

where $\hat{N}^* = 1 - \hat{v}_1 I_1^* - \hat{v}_2 I_2^*$, with I_1^*, I_2^* representing the first and second components of the vector.

The stability analysis of this model can be found in Mena-Lorca et al., 1995).

Figure Captions

Figure 1 v_2-σ parameter landscape of Model (1). We considered infection rates of the form $\beta_i = cv_i/(m+v_i)$. Parameter values are: $c = 5$, $v_1 = 0.5$, $m = 1$, and $u = 0.01$. The value of v_i is varied between 0.51 and 4; σ is varied between 0.01 and 2. For Model (1), the coordinates of the equilibrium are not defined for $\sigma = 0$. The boundary lines of the regions describe $I_1^* = 0$ and $I_2^* = 0$. In the shadowed area $0 < I_1^*, I_2^* \leq 1$. The plot was obtained using the command ContourPlot of *Mathematica* with the option PlotPoints set to 100. Further smoothing of boundary lines was obtained with Matlab.

Figure 2 1.) Numerical simulations of Model (1) with parameter values: $c = 5$, $v_1 = 0.5$, $m = 1$, $u = 0.01$, $\sigma = 0.25 < \sigma^*$ and $v_2 = 1.5$. The values of the (unstable) equilibrium coordinates are $I_1^* = 0.299048$ and $I_2^* = 0.272381$. 2.) Numerical simulations of Model (1) with the parameter values: $c = 5$, $v_1 = 0.5$, $m = 1$, $u = 0.01$, $\sigma = 0.9 > \sigma^*$ and $v_2 = 3.25$. The values of the (stable) equilibrium coordinates are $I_1^* = 0.349386$ and $I_2^* = 0.112446$. In both plots time units are arbitrary.

Figure 3 v_2-σ parameter landscape of Model (2). We considered infection rates of the form $\beta_i = cv_i/(m+v_i)$. Parameter values are: $c = 5$, $v_1 = 0.5$, $m = 1$, $k = 1$ and $u = 0.01$. The value of v_i is varied between 0.51 and 4; σ is varied between 0.01 and 2. The boundary lines of the regions describe $N^* = 0$, $I_1^* = 0$ and $I_2^* = 0$. In the shadowed area $0 < I_1^*, I_2^*, N^*$. The plot was obtained using the command ContourPlot of *Mathematica* with the option PlotPoints set to 100. Further smoothing of boundary lines was obtained with Matlab.

Figure 4 1.) Numerical simulations of Model (2) with parameter values: $c = 5$, $v_1 = 0.5$, $m = 1$, $u = 0.01$, $\sigma = 0.25$ and $v_2 = 1.5$. The values of the equilibrium coordinates are $I_1^* = 0.635083$ and $I_2^* = 0.204394$. 2.) Numerical simulations of Model (2) with the parameter values: $c = 5$, $v_1 = 0.5$, $m = 1$, $u = 0.01$, $\sigma = 1.2$ and $v_2 = 3.25$. The values of the equilibrium coordinates are $I_1^* = 0.138377$ and $I_2^* = 0.28113$. In both plots time units are arbitrary.

Figure 5 v_2-σ parameter landscape of Model (4). We considered infection rates of the form $\beta_i = cv_i/(m + v_i)$. Parameter values are: $b = 2$, $c = 5$, $v_1 = 0.5$, $m = 1$, and $u = 0.01$. The value of v_i is varied between 1 and 4; σ is varied between 0.01 and 1.4. The boundary lines of the regions describe $N^* = 0$, $I_1^* = 0$ and $I_2^* = 0$. In the shadowed area $0 < I_1^*, I_2^*, N^* \leq 1$. The plot was obtained using the command ContourPlot of *Mathematica* with the option PlotPoints set to 100. Further smoothing of boundary lines was obtained with Matlab.

Figure 6 1.) Numerical simulations of Model (4) with parameter values: $b = 2$, $c = 5$, $v_1 = 0.5$, $m = 1$, $u = 0.01$, $\sigma = 0.01$ and $v_2 = 2.47v_1$. The values of the equilibrium coordinates are $\hat{N}^* = 0.584017$, $I_1^* = 0.00200165$ and $I_2^* = 0.336018$. 2.) Numerical simulations of Model (4) with the parameter values: $c = 5$, $v_1 = 0.5$, $m = 1$, $u = 0.01$, $\sigma = 1$ and $v_2 = 5.3v_1$. The values of the equilibrium coordinates are $\hat{N}^* = 0.906135$, $I_1^* = 0.0942871$ and $I_2^* = 0.0176307$. In both plots time units are arbitrary.

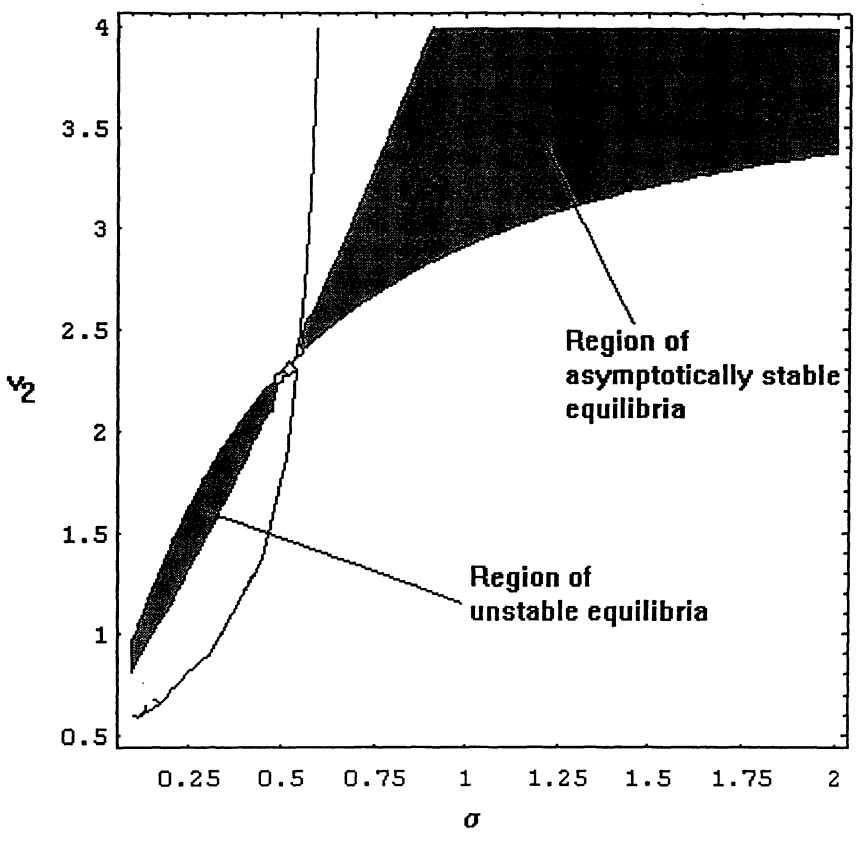
4
3.5
3
2.5
2
1.5
1
0.5
v_2
0.25
0.5
0.75
1
1.25
1.5
1.75
2
σ
Region of asymptotically stable equilibria
Region of unstable equilibria

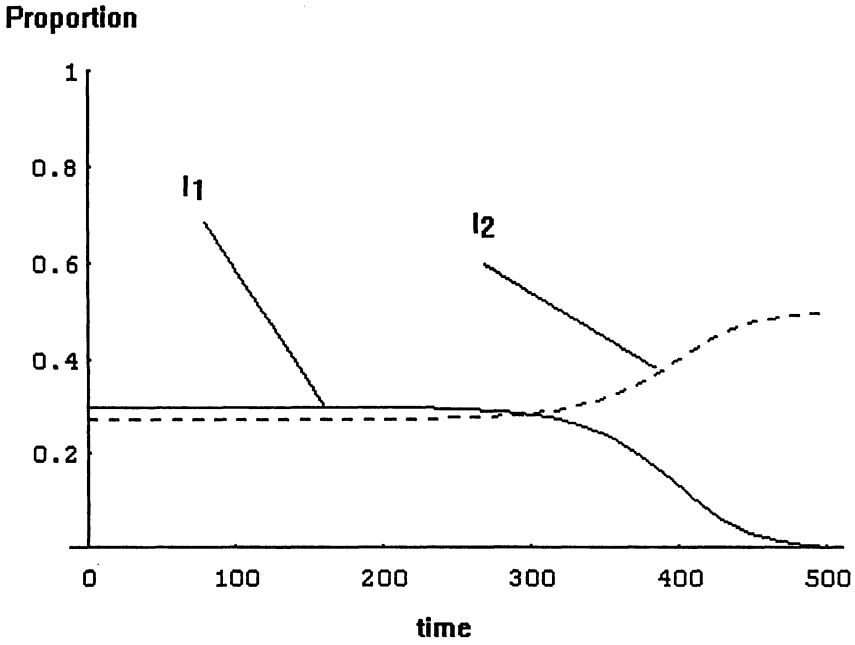
Proportion
1
0.8
0.6
0.4
0.2
I_1
I_2
0
100
200
300
400
500
time

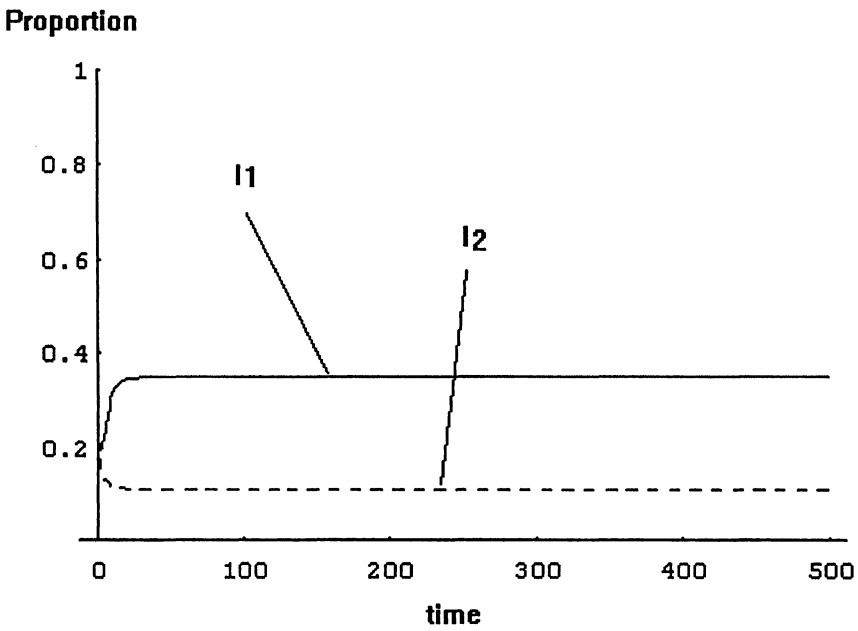

2.2

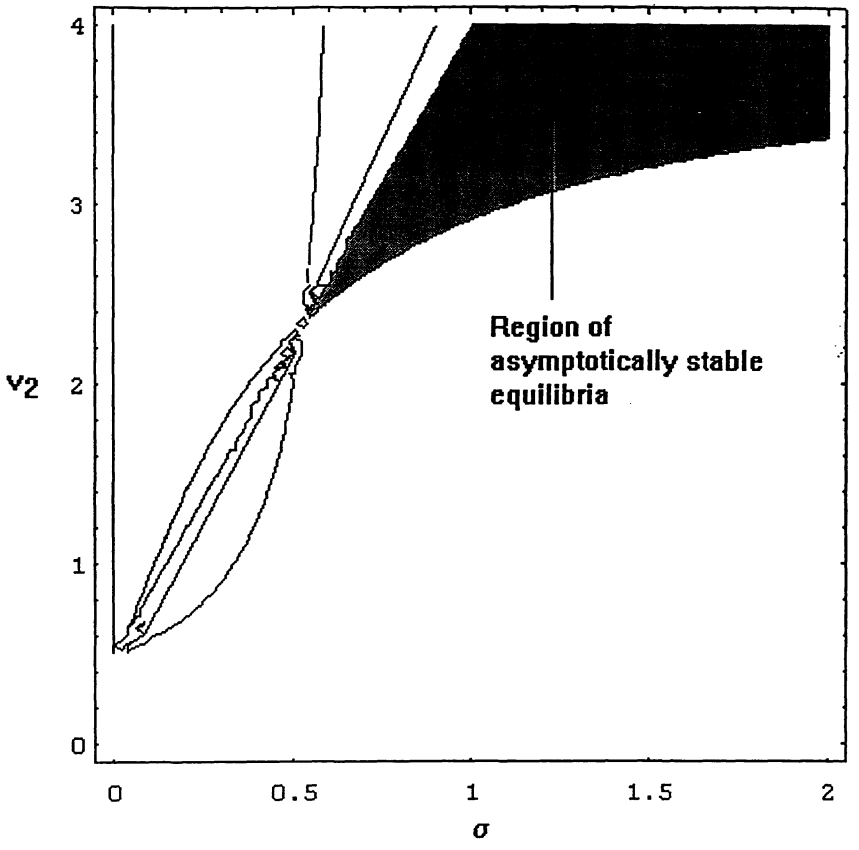
4
3
2
1
0
v_2
0
0.5
1
1.5
2
σ
Region of
asymptotically stable
equilibria

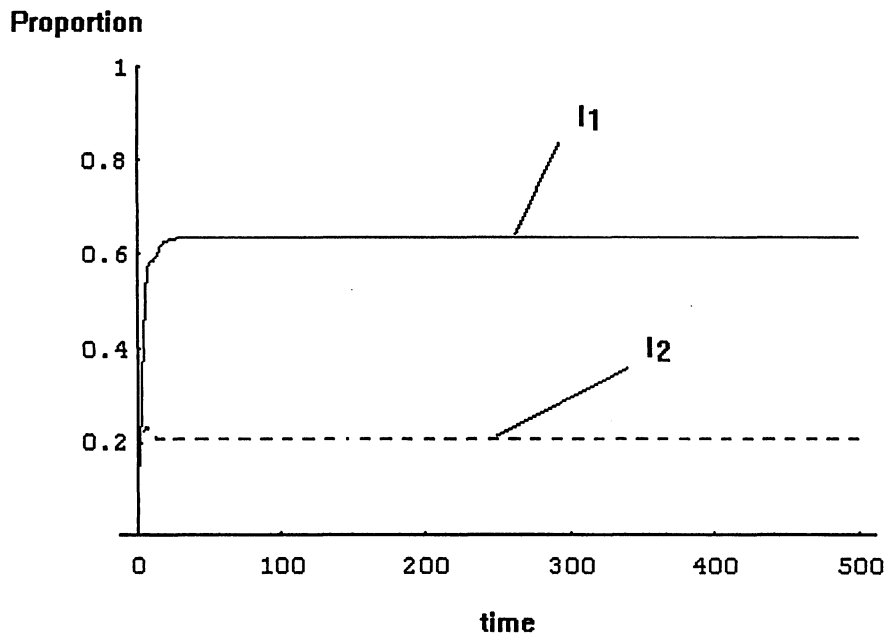

4.1 CR

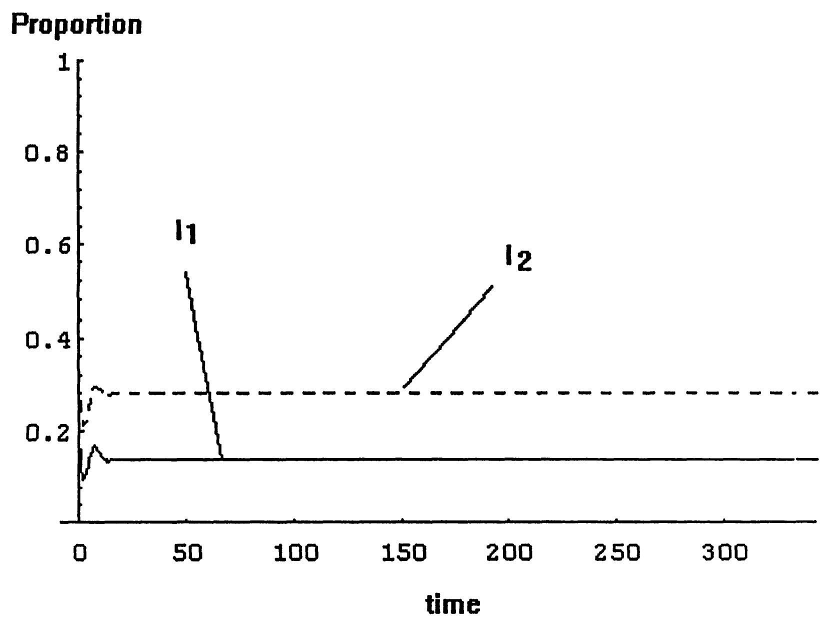

A.2 CR

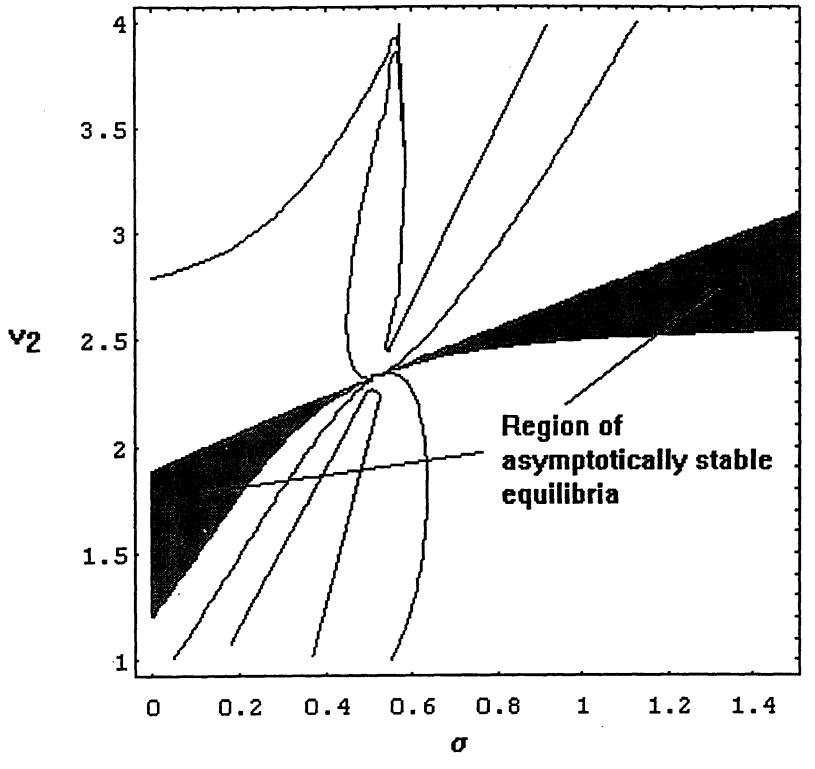
4
3.5
3
2.5
2
1.5
1
v_2
0
0.2
0.4
0.6
0.8
1
1.2
1.4
σ
Region of
asymptotically stable
equilibria

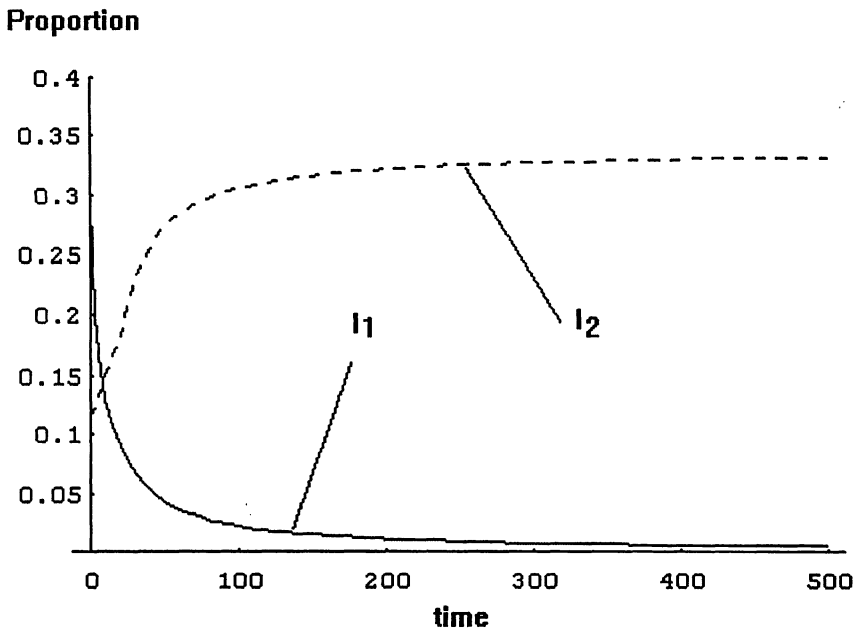
Proportion
0.4
0.35
0.3
0.25
0.2
0.15
0.1
0.05
0
100
200
300
400
500
time
I1
I2

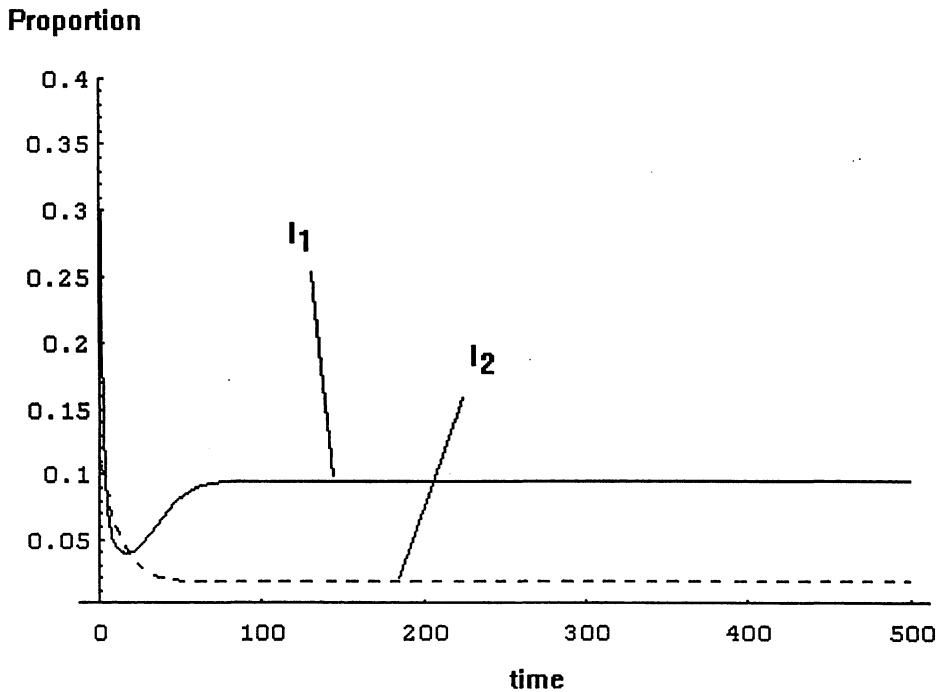
Proportion
0.4
0.35
0.3
0.25
0.2
0.15
0.1
0.05
I_1
I_2
0
100
200
300
400
500
time

6.2